Downslope Winds *

Dale R. Durran † University of Washington, USA

May 22, 2002

KEYWORDS: Downslope winds, Hydraulic theory

Introduction

Very strong surface winds sometimes develop when air flows over a high mountain ridge with a steep lee slope. Such winds are known to occur at many locations throughout the middle latitudes. Local names for these winds include the Alpine foehn, the Rocky Mountain chinook, the Croatian bora, the Santa Ana in southern California, and the Argentine zonda. These winds are collectively referred to as *downslope* winds. Downslope winds in the lee of major mountain barriers can approach hurricane strength. Every few years, for example, the eastern slope of the Colorado Front Range (part of the Rocky Mountains) experiences a damaging windstorm with peak gusts as high as 60 m s⁻¹ (216 km hr⁻¹). An anemometer trace recorded at the National Center for Atmospheric Research in Boulder, Colorado during a strong chinook is shown in Fig. 1.

In modern meteorological usage, downslope winds are distinguished from *kata-batic* winds by the dynamical processes driving each flow. Katabatic winds usually refer to shallow gravity currents generated by the cooling of surface air over sloping terrain. Downslope winds usually refer to winds generated as a deeper layer of air is forced over topography. In contrast to katabatic winds, the diabatic cooling of air in contact with a cold surface plays no essential role in the dynamics of downslope winds.

In most downslope wind events (including the typical foehn and chinook) the onset of the downslope wind is accompanied by an increase in the surface temperature and a drop in the dew point. Whereas the area of violent wind is limited to a relatively narrow swath along and adjacent to the lee slope, the warmer drier air mass can extend much further downstream. Nevertheless, in some cases the upstream conditions may be so cold, and the initial downstream conditions sufficiently warm, that the onset of a downslope wind brings a drop in temperature. The most well-known example

^{*}From the Encyclopedia of Atmospheric Sciences, 2003, pp. 644-650, Elsevier Science Ltd.

[†]Corresponding author: University of Washington, Atmospheric Sciences, Box 351640, Seattle, WA 98195-1640, USA.

 $^{^{1}}$ By definition, hurricanes are storms with *sustained* winds of at least 32 m s⁻¹ (115 km h⁻¹).

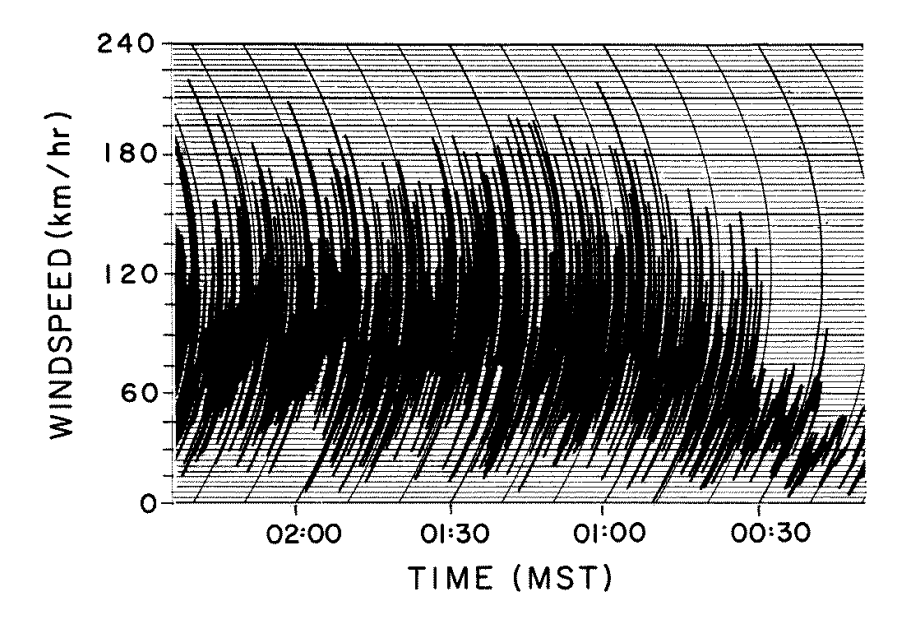


Figure 1: Anemometer trace recorded at the National Center for Atmospheric Research during the onset of the 17 January 1982 Boulder windstorm. Time reads right to left. (After Fig. 4.11 of Durran 1990).

of this type of cold downslope wind is the Croatian bora. Despite the difference in the evolution of the surface temperature, there does not appear to be any significant dynamical distinction between the processes responsible for the development of high downslope winds in cold and warm events.

Contours of the potential temperature observed on 11 January 1972 during an intense downslope windstorm are plotted in the vertical cross-section through Boulder, Colorado shown in Fig. 2. These contours provide a rough indication of the streamlines in the flow, which is moving from left to right. (The isentropes would be exactly identical to streamlines if the flow were steady, inviscid, adiabatic and two-dimensional). A large-amplitude mountain wave is clearly visible in the potential temperature field just to the lee of the continental divide. The apparent horizontal displacement of the wave trough at upper levels from its position at low levels is due to a two-hour difference between the times at which observations were collected in the upper and lower flight levels. Also apparent in Fig. 2 is a layer of enhanced static stability around the 550 mb level in the upstream flow. When intense downslope winds develop in a deep cross-mountain flow, strong mountain waves and low-level stable layers similar to those shown in Fig. 2 are usually present.

The connection between mountain waves and strong downslope winds is less apparent in situations where the cross-mountain wind component reverses with height at some level in the middle or lower troposphere, as is often the case in the Croatian bora or when strong winds blow from the east down the western slopes of the Wasatch mountains in Utah. Contours of the potential temperature observed during a moderate

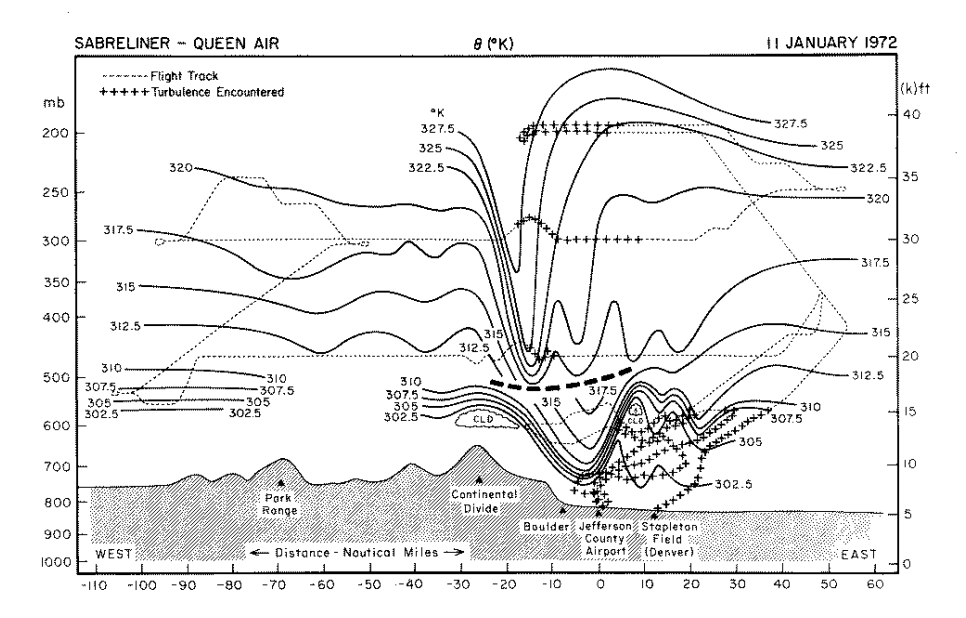


Figure 2: Cross section of potential temperature along an east-west line through Boulder, Colorado from aircraft observations collected on 11 January 1972. The heavy dashed line separates data collected by two aircraft at different times. Flight tracks are indicated by the dotted lines; those segments along which significant turbulence was encountered are denoted by pluses. (After Fig. 7 of Lilly 1978.)

bora along a cross section through Senj, Croatia are shown in Fig. 3. The flow in this example is from right to left. A low-level inversion is once again apparent upstream of the mountains; however, no significant wave activity is present above the 3-km level. In this case the upstream inversion is coincident with a region of strong vertical wind shear in which the cross-mountain wind component reverses direction. The level at which the cross-mountain wind component drops to zero is a critical level² for steady two-dimensional mountain waves, and any gravity waves triggered by the mountain break down and dissipate as they approach this critical level.

The hydraulic analog

The dynamics governing the development of strong downslope winds in the atmosphere are analogous to those governing the rapid increase in speed that occurs when water flowing over a rock in a river undergoes a transition from a relatively slow velocity upstream to a thin layer of high-velocity fluid over the downstream face. In such circumstances, a turbulent hydraulic jump often develops downstream of the rock at the point where the high-speed flow decelerates back to the ambient velocity of the river.

²A critical level is a level at which the phase speed of a wave equals the speed and direction of the basic-state flow.

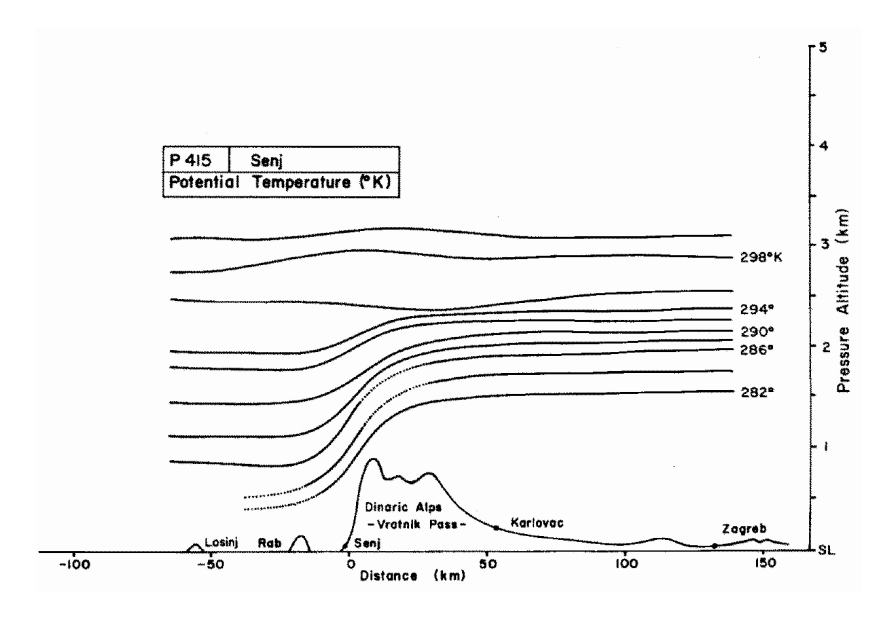


Figure 3: Cross section of potential temperature along a northeast-southwest line through Zagreb and Senj, Croatia. (After Fig. 9b of Smith 1987).

Since the fundamental processes responsible for the rapid acceleration of water flowing over a rock can be explained more simply than those which govern downslope winds in the atmosphere, let us begin by considering the hydraulic model for a shallow layer of water flowing over an obstacle in an open channel.

Suppose a homogeneous fluid, such as fresh water, is flowing over a ridge-like obstacle. Assuming the flow is steady and that there are no variations in the coordinate direction parallel to the ridge axis, and making the hydrostatic approximation, the flow is governed by the horizontal momentum equation

$$u\frac{\partial u}{\partial x} + g\frac{\partial D}{\partial x} = -g\frac{\partial h}{\partial x},\tag{1}$$

and the mass continuity equation

$$\frac{\partial uD}{\partial x} = 0, (2)$$

where x is the horizontal coordinate directed perpendicular to the ridgeline, u is the velocity in the x direction, D is the thickness of the fluid, and h is the local height of the obstacle. Using (2) to substitute for $\partial u/\partial x$ into (1) yields

$$(1 - F^{-2}) \frac{\partial}{\partial x} (D + h) = \frac{\partial h}{\partial x}.$$
 (3)

Here

$$F = \frac{u}{\sqrt{gD}},\tag{4}$$

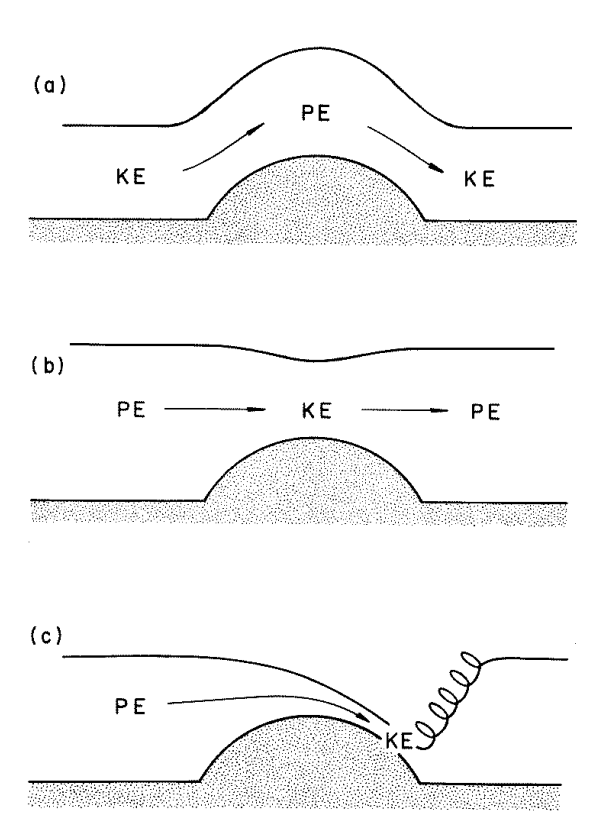


Figure 4: Behavior of shallow water flowing over an obstacle: (a) everywhere supercritical flow, (b) everywhere subcritical flow, (c) hydraulic jump after a transition from supercritical to subcritical flow over the crest. (After Fig. 4.5 of Durran 1990).

is the Froude number, which is the ratio of the local flow speed to the local phase speed of a linear shallow-water gravity wave.

According to (3), the magnitude of the Froude number determines whether the free surface rises or falls as the fluid ascends the upstream slope of the obstacle. The case F>1, known as *supercritical flow*, is shown in Fig. 4a; the fluid thickens and slows as it passes over the top of the obstacle, and it reaches its minimum speed at the crest. The accelerations experienced by the fluid are qualitatively similar to those experienced by a hockey puck traversing a frictionless ridge of ice. The case F<1, known as *subcritical flow*, is shown in Fig. 4b. The fluid-parcel accelerations in the subcritical flow seem counterintuitive in that the fluid thins and accelerates as it crosses the top of the obstacle, reaching its maximum speed at the crest.

Why does a subcritical flow accelerate as it encounters rising bottom topography? In contrast to a frictionless hockey puck, the acceleration of a fluid parcel is determined not only by gravity and by the angle of the slope, but also by pressure gradient forces. The steady-state momentum equation (1) requires a three-way balance between acceleration (the first term), pressure gradient forces arising from changes in the fluid

depth (the second term), and the work per unit mass per unit horizontal distance done against gravity while ascending the sloping topography (the third term). The value of the Froude number determines whether the work done against gravity is predominately balanced by accelerations or by the pressure gradient force. From (2)

$$\left(u\frac{\partial u}{\partial x}\right) / \left(g\frac{\partial D}{\partial x}\right) = \left(u\frac{\partial u}{\partial x}\right) / \left(-\frac{gD}{u}\frac{\partial u}{\partial x}\right) = -F^2.$$
(5)

Thus in steady open-channel hydraulic flow, acceleration always opposes the pressure gradient force due to changes in fluid depth. Furthermore F^2 may be interpreted as the ratio of the magnitude of the acceleration to the magnitude of the pressure gradient force generated by changes in the fluid depth. In supercritical flow (F>1) acceleration dominates the pressure gradient force and the three-way balance in (1) is satisfied such that fluid parcels ascending the upstream slope decelerate as they do work against gravity.

Before discussing the subcritical case, it is helpful to recast the discussion in terms of the conversions between kinetic energy (KE) and potential energy (PE). Equation (1) implies that $u^2/2+g(D+h)$ is constant along a streamline. This is just Bernoulli's theorem for steady incompressible hydrostatic flow since the contribution of $w^2/2$ to the total kinetic energy is neglected in the hydrostatic approximation. The term g(D+h) represents the combined potential energies associated with the gravitational and pressure fields, as may be verified by taking the hydrostatic pressure to be zero at the top of the water and choosing the z=0 level to coincide with the bottom of the channel away from the obstacle; then at an arbitrary level z,

$$gz + \frac{p}{\rho_0} = gz + g(D + h - z) = g(D + h).$$
 (6)

According to this generalized interpretation of potential energy, fluid parcels ascending the obstacle in a supercritical flow slow down as they convert kinetic energy (KE) to potential energy (PE), and after passing the crest they reaccelerate as PE is converted back to KE (Fig. 4a).

On the other hand, in subcritical flow (F < 1) the pressure gradient force dominates acceleration and the three-way balance in (1) requires that fluid parcels accelerate in the direction opposite to the component of gravity parallel to the topography. As shown in Fig. 4b, fluid parcels ascending the obstacle accelerate as the free surface drops and PE is converted to KE. After passing the crest, the parcels decelerate as KE is converted back to PE. The disturbance centered over the obstacle in Fig. 4b is a steady surface gravity wave.

The flow regime that serves as an analog for downslope windstorms is shown in Fig. 4c. If the flow is subcritical upstream and if a column of fluid undergoes a sufficient acceleration and experiences a sufficient decrease in thickness as it ascends toward the crest, a transition from subcritical to supercritical flow occurs at the top of the obstacle. Since the lee-slope flow is now supercritical, fluid parcels continue to accelerate as they descend, and very high velocities can be produced because PE is converted to KE during the entire time over which a fluid parcel traverses the obstacle. The deceleration that would otherwise occur in the lee-side portion of the standing

gravity wave is disrupted when the flow becomes supercritical. In this case fluid parcels eventually decelerate when they pass through a turbulent hydraulic jump at some point downstream from the crest.

Application of the Hydraulic Analog to the Atmosphere

The hydraulic analog is best applied to the atmosphere in a qualitative, rather than an quantitative, manner. Quantitative application is hindered by the difficulty of defining a dynamically meaningful Froude number in vertically unbounded continuously stratified flow. A variety of expressions have been described as Froude numbers in the literature, but all of the simple expressions have serious deficiencies.

The parameter $U/(Nh_0)$, where N is the Brunt-Väisälä frequency, U the wind speed, and h_0 is the maximum mountain height, is sometimes referred to as the Froude number in idealized cases in which N and U are constant throughout the upstream flow. Unlike the denominator in the conventional shallow-water Froude number, Nh_0 is not the horizontal phase speed of any particularly significant wave. On the other hand, the maximum perturbation horizontal wind speed u' in linear flow over an obstacle with constant N and U scales like Nh_0 , so that $U/(Nh_0) \approx U/u'$ might be better described as a nonlinearity parameter.

When there is a strong well-defined inversion at some elevation H in the upstream flow, many authors have attempted to define a Froude number as $U/\sqrt{g'H}$, where $g'=g\Delta\theta/\theta_0$ is the "reduced gravity," $\Delta\theta$ is the increase in potential temperature across the inversion, and θ_0 is the mean potential temperature below the inversion. The difficulty with this approach is that it implies that the pressure gradient force is entirely determined by the vertical displacements of the inversion layer and thereby neglects the influence, on the surface pressure gradient, of vertical displacements in the stably stratified fluid above and below the inversion. Moreover, it is also very difficult to determine a precise quantitative value for $U/\sqrt{g'H}$ in more general applications in which the wind speed is not constant below the inversion and the inversion itself may be indistinct. As a consequence, the reduced-gravity shallow-water model, in which F is replaced by $U/\sqrt{g'H}$ in (3), will not reliably yield reasonable approximations to the speed and depth of the downslope flow in actual windstorms.

Significant downslope winds have been observed to develop in three basic situations: (1) when a standing mountain wave in a deep cross-mountain flow achieves sufficient amplitude to overturn and breakdown at some level in the troposphere, (2) when standing mountain waves break and dissipate at a critical level in a shallow cross-mountain flow, and (3) when there is sufficient static stability near mountain-top level in the cross-mountain flow to create high downslope winds even without wave breaking. The qualitative application of hydraulic theory to the dynamics of downslope winds centers on the idea that in all three of these cases there is a transition from wave-like behavior over the upstream slopes of the topography to a non-wave-like regime in the lee.

 $^{^3}Nh_0$ is the phase speed of a hydrostatic internal gravity wave with vertical wavelength $2\pi h_0$, but there is nothing particularly significant about this wavelength in contrast to other similar waves with wavelengths such as $5h_0$ or $6h_0$.

First consider the case of breaking waves in a deep cross-mountain flow. The structure of the low-level horizontal velocity perturbations in a stationary 2D internal gravity wave forced by an isolated ridge are shown in Fig. 5a. In this case the upstream wind

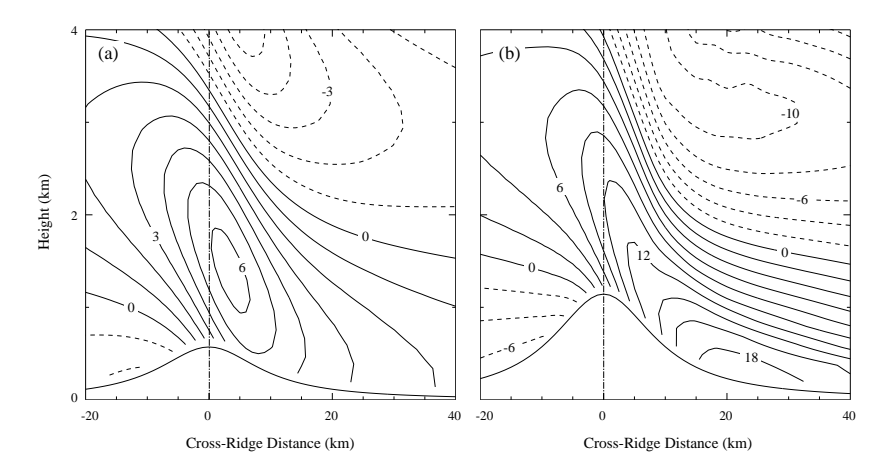


Figure 5: Perturbation horizontal velocity in flow over an isolated mountain when: (a) $Nh_0/U=0.6$, contour interval 1 m s⁻¹ and (b) $Nh_0/U=1.2$, contour interval 2 m s⁻¹.

and static stability are constant with height such that $N=0.01047~\rm s^{-1}$, $U=10~\rm m~s^{-1}$, and $Nh_0/U=0.6$. Streamlines for this same stationary internal gravity wave are plotted in Fig. 3a of the entry *Lee Waves and Mountain Waves*. As apparent in Fig. 5a, the detailed structure of the velocity perturbations in the internal gravity wave are somewhat different from those in the surface gravity wave schematically illustrated in Fig. 4b. In particular the maximum perturbation surface wind speed occurs halfway down the lee slope in the internal gravity wave, whereas it occurs at the crest in the surface gravity wave. Nevertheless, both types of waves allow a fluid parcel to arrive at the ridge crest with a positive perturbation velocity (i.e., to undergo a net acceleration while ascending to the crest), and in both cases the wind speed eventually returns to its ambient value well downstream of the crest as KE is converted back to PE in the lee-side portion of the stationary gravity wave.

The enhancement of the perturbation horizontal winds along the lee slope in Fig. 5a is too weak to create significant downslope winds. (The total wind speed increases from $10 \,\mathrm{m\,s^{-1}}$ far upstream to approximately $15 \,\mathrm{m\,s^{-1}}$ in the lee.) Much stronger downslope winds occur in the case shown in Fig. 5b, which is a vertical cross section of the perturbation horizontal velocity in a simulation identical to that shown in Fig. 5a, except that the height of the mountain has been doubled so that $Nh_0/U=1.2$. The higher topography in this case forces the internal gravity wave to overturn and produces a well mixed region of weakly reversed flow at elevations around 3 km over the lee slope. (The region of reversed flow is that in which the horizontal perturbation velocity is less that -10 m s⁻¹.) Streamlines for this same wave-breaking case are shown in Fig. 4a of the entry *Lee Waves and Mountain Waves*. Although the lee-side flow is dramatically

different when the wave is breaking, the flow upstream of the crest remains consistent with that in a stationary internal gravity wave. Linear theory for stationary internal gravity waves predicts that doubling the mountain height should double the amplitude of the perturbation horizontal velocities without changing the spatial distribution of the perturbations relative to the mountain, and this is essentially the case in the region upstream of the crest. Note, for example, the similarity of the 3 m s⁻¹ contour in Fig. 5a to the 6 m s⁻¹ contour in Fig. 5b.

Since the wave in Fig. 5b has become unstable and overturned above the lee slope, there is no standing gravity wave to decelerate the fluid parcels as they descend. Instead these parcels continue to accelerate as PE is converted to KE along the entire lee slope, generating strong downslope winds in which the maximum surface wind speeds (> 28 m s⁻¹) are approximately three times stronger than the 10 m s⁻¹ flow far upstream. Wave breaking in a deep cross-mountain flow appears to have played an important role in the generation of the 11 January 1972 Boulder, Colorado windstorm. The presence of breaking waves is suggested by the almost vertical orientation of the isentropes on the lee side of the trough in the upper-level wave in Fig. 2 and by the turbulence encountered along the flight legs through this region.

The second type of situation conducive to the development of strong downslope winds is illustrated in Fig. 3. In this bora event a critical level at an elevation of about 2 km disrupts the lee-side gravity wave so that once again, fluid parcels near the surface undergo a net acceleration in the wave-like upstream flow as they ascend to the mountain crest and then continue to accelerate as they convert PE to KE while descending the entire lee slope. The vertical displacement of a streamline about its initial undisturbed level $\delta(x,z)$ can be modeled with reasonable fidelity in the flow beneath the critical layer by solving the hydrostatic Long's equation

$$\frac{\partial^2 \delta}{\partial z^2} + \frac{N^2}{U^2} \delta = 0, \tag{7}$$

subject to the lower boundary condition that the streamline follow the topography,

$$\delta[x, z = h(x)] = h(x) \tag{8}$$

and an upper boundary condition in which the horizontal wind speed is held constant along a "dividing streamline" separating the well-mixed turbulent region from the underlying high-speed flow. In the case shown in Fig. 3, the 294 K isentrope approximates a dividing streamline while the 296 K isentrope roughly coincides with the top of the wedge of well mixed air downwind of the crest. Very close mathematical analogies exist between conventional shallow-water hydraulic theory and the mathematical solutions to (7)–(8), although there is no *simple* parameter that plays the role of the Froude number in this analogy.

The third situation that produces strong downslope winds may occur when there is high static stability at low-levels in the cross-mountain flow and lower stability aloft. A prototypical example of this type is presented in Fig. 6, which shows contours of the perturbation horizontal velocity field and streamlines from a numerical simulation identical to that described in Fig. 5a, except that the Brunt-Väisälä frequency above 3 km in the upstream flow is reduced by a factor of 0.4. Comparison of the horizon-

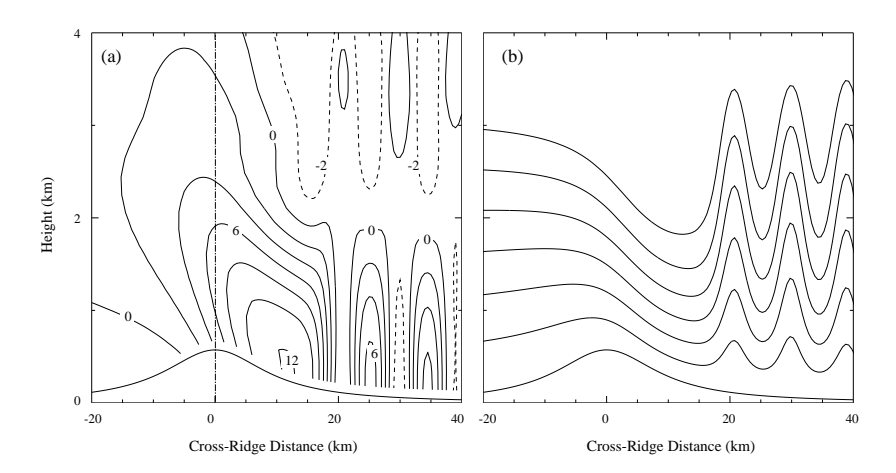


Figure 6: Two-layer flow over an isolated mountain in which the upstream value of Nh_0/U is 0.6 in the lower layer and 0.24 above: (a) perturbation horizontal velocity, contour interval 2 m s⁻¹, (b) streamlines within the lower layer.

tal wind speed perturbations between Fig. 5a and Fig. 6a shows that the perturbation horizontal winds are twice as strong and that the maximum winds have shifted to the surface along the lee slope in the two-layer flow. The amplification of the surface winds in the two-layer simulation is produced without wave breaking; in fact the flow does not come close to stagnation.

The streamlines within the lower layer shown in Fig. 6b appear similar to those in water undergoing a transition from subcritical to supercritical flow over the crest of an obstacle. Near the base of the lee slope in Fig. 6, the flow recovers toward ambient conditions by radiating energy downstream in a series of vertically trapped gravity waves. The removal of energy by these trapped waves is analogous to the dissipation of energy at the point where the flow recovers toward ambient downstream conditions in a hydraulic jump in the standard shallow-water model (Fig. 4c). Additional sensitivity studies have demonstrated that the changes in the depth of the lower layer and the maximum height of the mountain modify the two-layer flow in a manner one would expect on the basis of hydraulic theory. In particular, making the lower layer too deep or the mountain too small eliminates the transition to a high wind regime.

In actual downslope wind events the dynamical influence of a low-level stable layer may act in concert with wave breaking to generate very high winds. Indeed climatological data and numerical experiments suggest this is often the case in Boulder windstorms. In particular, nonlinear wave amplification due to the presence of a low-level stable layer appears to have served as a necessary precursor to wave breaking during the 11 January 1972 event.

See also: Katabatic winds, Mountain waves, Buoyancy waves, Lee Vortices

References

[1] D. R. Durran. Mountain waves and downslope winds. In William Blumen, editor, *Atmospheric Process over Complex Terrain*, pages 59–81. American Meteorological Society, Boston, 1990.

- [2] D. K. Lilly. A severe downslope windstorm and aircraft turbulence event induced by a mountain wave. *J. Atmos. Sci.*, 35:59–77, 1978.
- [3] R. B. Smith. Aerial observations of the Yugoslavian bora. *J. Atmos. Sci.*, 44:269–297, 1987.
- [4] R. B. Smith. Hydrostatic airflow over mountains. In B. Saltzman, editor, *Advances in Geophysics*, volume 31, pages 1–41. Academic Press, 1989.